CAMPO MAGNETICO TERRESTRE E TERREMOTI

Antonio Meloni, INGV Roma

L'Aquila, 26-28/4/2010

Intorno ai fenomeni elettrici e magnetici precedenti, concomitanti e susseguenti i terremoti molto si è discusso e molto si discute tuttora: di essi da taluno fu esagerata la importanza facendo dell'elettricità la causa efficiente ai terremoti stessi…

Da Mario Baratta, *CATALOGO DEI FENOMENI ELETTRICI E MAGNETICI APPARSI DURANTE I PRINCIPALI TERREMOTI, 1891*

The Earth is surrounded by a magnetic field. When, at a given point and at a certain time, a measurement of the Earth's magnetic field is carried out, the measured value is the result of the superimposition of contributions having different origins.

A) The main field, generated in the Earth's fluid core by a geodynamo mechanism;

B) The crustal field, generated by magnetized rocks in the Earth's crust;

C) The external field, produced by electric currents flowing in the ionosphere and in the magnetosphere, owing to the interaction of the solar electromagnetic radiation and the solar wind with the Earth's magnetic field;

D) The magnetic field resulting from an electromagnetic induction process generated by electric currents induced in the crust and the upper mantle by the external magnetic field time variations.

SOURCES AND SPACE SCALES OF CONTRIBUTIONS TO THE EARTH'S MAGNETIC VARIATIONS

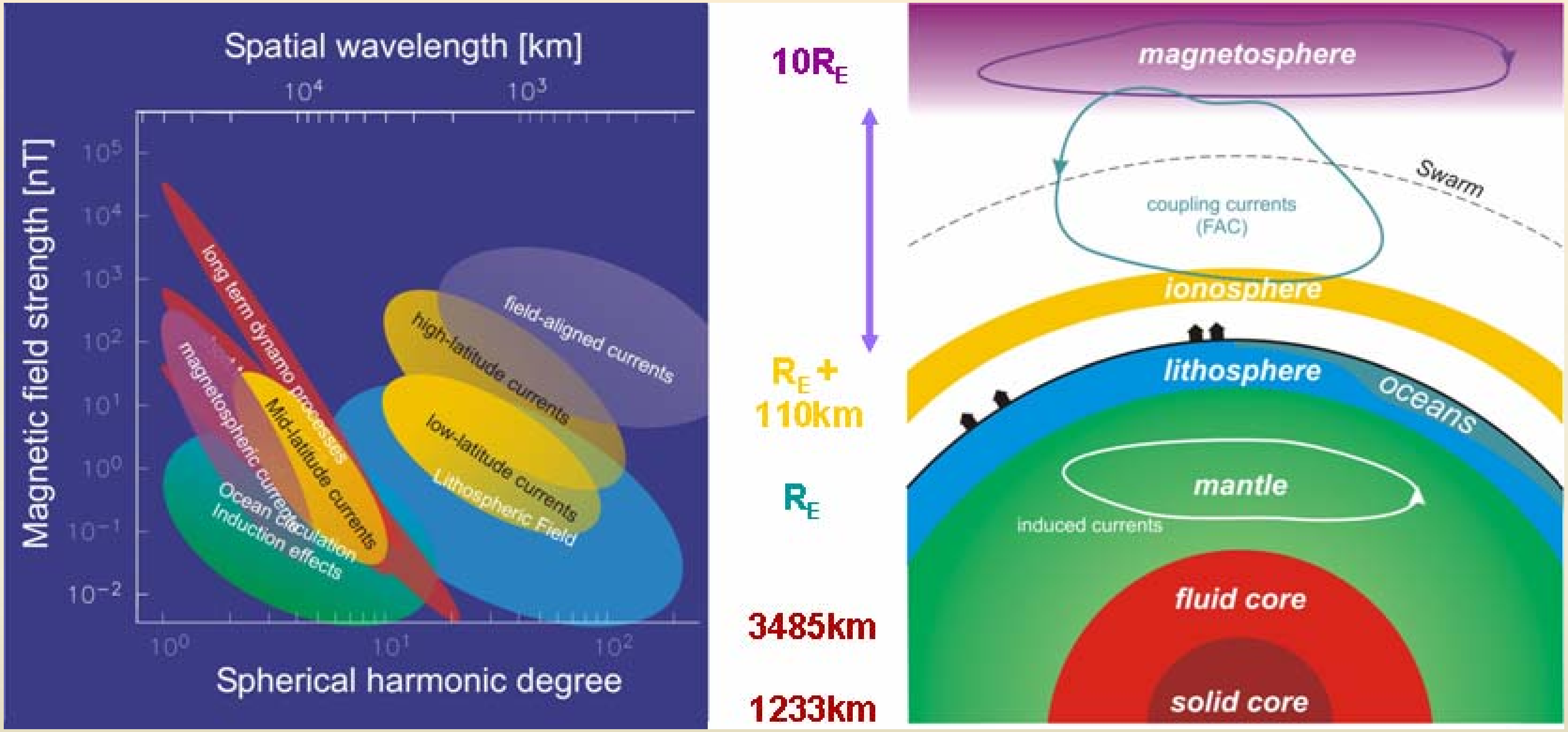

EARTH'S MAGNETIC FIELD TIME VARIATIONS AND RELATED INFORMATION

		DENOMINATION	SOURCE LOCATION	MAXIMUM INTENSITY	MORPHO LOGY	CHARACTERI STIC TIME	VARIATION ORIGIN	DETECTION
INTERNAL EARTH CONTRIBUTION		**MAIN FIELD**	**FLUID CORE** (1230- 3500 km from Earth's center)	**Average 45000-nT** (25000 to70000 nT)	**DIPOLAR + MULTIPOLAR**	Existing since 4 Gyears POLARITY REVERSALS ($10^5 10^6$ YEARS) **SECULAR VARIATION** (T > 1-100/nT YEAR)	**ELECTRICAL CURRENTS AND (MHD) WAVES IN CONVECTIVE AND TURBOLENT REGIME IN THE FLUID CORE**	**SURVEYS** (GEOMAGNETIC OBSERVATORIES, SHIPS AEROMOBILE AND SATELLITE SURVEYS) ROCK MAGNETISM
		LOCAL FIELD	**EARTH'S CRUST** down to Curie point temeperature depths	**200 nT** (AVERAGE WITH MAXIMA AROUND 10^4 nT)	Mainly locally dipolar and **IRREGULAR** (down to scales of a few m)	**Oldest magnetized rocks 3.8 Gyears Stable on Geological time scale**	**Ferromagnetic minerals and magnetic induction in the crust**	**LOCAL SURVEYS** SHIP AEROMOBILE AND SATELLITE SURVEYS) ROCK MAGNETISM
EXTERNAL EARTH CONTRIBUTION	IRREGULAR TIME VARIATIONS	**MAGNETIC STORM**	**MAGNETOSPHERIC CURRENTS**	**Dst 100-200 nT** (500 nT max)	**FIELD UNIFORM ON A GLOBAL SCALE, LATITUDE DEPENDENT**	**FROM 4 TO 12 HOURS; RECOVERY PHASE GOES FROM 1 TO 3 DAYS**	**SOLAR WIND INTERACTION WITH MAGNETOSPHERIC AND IONOSPHERIC PLASMA**	
		SUBSTORMS (BAYS AT MID LATITUDES)	**IONOSPHERIC AND FIELD ALIGNED ELECTRIC CURRENTS**	**100 nT** (200 nT IN AURORAL ZONE	**UNIFORM ON A LOCAL SCALE STRONGLY LATITUDE DEPENDENT**	**5 TO 100 MINUTES**	**SOLAR WIND INTERACTION WITH MAGNETOSPHERIC AND IONOSPHERIC PLASMA**	**GEOMAGNETIC OBSERVATORY MAGNETOGRAMS, TEMPORARY STATIONS AND SATELLITES**
		PULSATIONS Continuous / Irregular	**MHD MAGNETOSPHERIC WAVES AND CURRENTS FIELD LINE OSCILLATIONS**	**Few nT** (max100 nT in AURORAL ZONE	**ALMOST UNIFORM FILD, MORE INTENSE IN AURORAL ZONES Quasi periodic**	**Pc1: 0.2-5 sec Pc2: 5-10 sec Pc3: 10-45 sec Pc4: 45-150 sec Pc5: 150-600 sec Pi1: 1-40 sec Pi2: 40-150 sec Pg : Giant Pulsations**	**FILED LINES RESONANCE IN MAGNETOSPHERE**	
	REGULAR TIME VARIATIONS	**DIURNAL VARIATION**	**TIDAL IONOSPHERIC CURRENTS**	**50-100 nT** (200 Nt in equatorial zone)	**UNIFORM FIELD MORE INTENSE IN EQUATORIAL ZONE**	**T = 24, 12, 8, 6 HOURS**		
		SOLAR	**photoionization**	**10-50 nT**	**UNIFORM**	**STRONG SEASONAL AND SOLAR CICLE CONTROL**	**IONOSPHERIC TIDES**	**GEOMAGNETIC OBSERVATORY MAGNETOGRAMS,**
		LUNAR	**Atmospheric tides**	**2-5 nT**	**UNIFORM**	**T = 24h 50m LUNAR**		
INTERNAL EARTH SECONDARY CONTRIBUTION		**EM INDUCTION BY EXTERNAL TIME VARIATION**	**CONTINENTAL AND OCEANIC CRUST AND UPPER MANTLE**	**SMALLER AMPLITUDE THAN PRIMARY; MAINLY IN Z**	**UNIFORM WITH IRREGULAR MORPHOLOGY**	**SIMILAR TO EXTERNAL PRIMARY, PHASE SHIFTS**	**ELECTROMAGNETICil INDUCTION BY PRIMARY EXTERNAL TIME VARIATIONS**	**GEOMAGNETIC OBSERVATORY MAGNETOGRAMS, TEMPORARY STATIONS**

Seismo-electromagnetic effects refer to electromagnetic fields generated by fault failure processes in the Earth's crust

The loading and rupture of water-saturated crustal rocks during earthquakes, together with fluid/gas movement, stress redistribution, and change in material properties, is expected to generate associated magnetic and electric field perturbations.

The detection of related perturbations prior to fault rupture is proposed frequently as a simple and inexpensive method to monitor the state of crustal stress and perhaps to provide tools for predicting crustal failure.

The primary mechanisms for generation of electric and magnetic fields with crustal deformation and earthquake related fault failure, include

piezomagnetism
stress/conductivity
electrokinetic effects
charge generation processes, charge dispersion
magnetohydrodynamic effects
thermal remagnetization and demagnetization effects.

An overview of all these mechanisms and some related observations follows…

PIEZOMAGNETISM

Magnetic properties of rocks, under laboratory conditions, were shown to depend on the state of applied stress. Theoretical models were developed in terms of single domain and pseudo-single domain rotation and multidomain wall translation. The fractional change in magnetization per unit volume as a function of stress, is generally expressed in the form;

$$\Delta I \approx K\sigma \cdot I$$

where $\boldsymbol{\Delta I}$ is the change in magnetization in a body with net magnetization $\boldsymbol{I}$ due to a deviatoric stress σ (K, stress sensitivity, has values of about 3 x10^{-3} MPa^{-1}). The surface field (B_P) at a point, P, can be calculated in two ways: (1) by either integrating the change in magnetization I_Q in a unit volume, dv, at a point Q where the stress is σ_{ij}, and r is the distance between P and Q, according to (Stacey)

$$\Delta B_P = -\frac{\mu}{4\pi}\nabla \int_V \Delta I_Q \cdot \frac{r}{r^3}\, dv$$

Or by a method introduced by Sasai. Analytic expressions of the surface piezomagnetic potential, W, produced by a known stress distribution in a magnetoelastic half-space are obtained by transforming the stress matrix and integrating over the magnetized region. In this latter case, the surface field can be found from:

$$\Delta B_P = -\nabla W$$

These models show that magnetic anomalies of a few nanoteslas (nT) should be expected to accompany earthquakes for rock magnetizations and stress sensitivities of 1 A m^{-1} and 10^{-3} MPa^{-1}, respectively.

These magnetic signals are occasionally observed with the correct sign and amplitude.

STRESS/RESISTIVITY AND STRAIN/RESISTIVITY EFFECTS

Electrical resistivity of rocks also depends on stress (as demonstrated in laboratory). Resistivity in low porosity crystalline rock increases with compression as a result of crack closure at about 0.2%/bar and decreases with shear due to crack opening at about 0.1%/bar. More porous rocks have even lower stress sensitivity. Moreover the situation is complicated since non-linear strain can also produce resistivity changes.

A stress/resistivity relation for homogeneous material has the scalar form:

$$\frac{\Delta\rho}{\rho} \approx K_r \sigma$$

where $\boldsymbol{\rho}$ is resistivity, ***Kr*** is a constant, and $\boldsymbol{\sigma}$ is the stress. Unfortunately, the Earth is not homogeneous and many factors including rock type, crack distribution, degree of saturation, porosity, strain level, etc., can localize or attenuate current flow.

This equation provides only a starting point for calculating resistivity changes near active faults.

Measurements of resistivity change are made with both active experiments or passive telluric and magnetotelluric (MT) experiments

In the latter case changes in resistivity are inferred from changes in telluric or MT transfer functions.

Field observations of stress changes accompanying earthquakes (1 MPa), resistivity suggest that changes of at least 1% in resistivity might be expected to accompany crustal failure.

ELECTROKINETIC EFFECTS

Electrokinetic electric and magnetic fields result from fuid flow through the crust in the presence of an electric double layer at the solid-liquid interfaces. This double layer consists of ions anchored to the solid phase, with equivalent ionic charge of opposite sign distributed in the liquid phase near the interface.

Fluid fow in this system transports the ions in the fluid in the direction of flow, and electric currents result. Conservation of mass arguments supported by surface strain observations limit this process in extent and time because large-scale fuid fow cannot continue for very long before generating easily detectable surface deformation.

The current density ***j*** and fluid flow ***v*** are found from coupled equations given by

$$j = -s\nabla E - \frac{\xi\zeta\nabla P}{\eta}$$

$$v = \frac{\phi\xi\zeta\nabla E}{\eta} - \frac{\kappa\nabla P}{\eta}$$

Back   Impresse   Currents

where ***E*** is streaming potential, ***s*** is the electrical conductivity of the fluid, ***ξ*** is the dielectric constant of water, ***η*** is fuid viscosity, (***ς*** is the zeta potential, ***φ*** is the porosity, ***κ*** is the permeability, and ***P*** is pore pressure) .

The current density in Equation has two components. The second term represents electric current resulting from mechanical energy being applied to the system and is sometimes called the ‘impresse’ current. This term describes current generated by fluid flow in fractures. The first term of Eq. represents ‘back’ currents resulting from the electric field generated by the fluid flow.

The distribution of electrical conductivity determines the net far-field magnetic and electric fields resulting from these effects.

In an extreme case, if the fluid is extremely conducting and the surrounding region is not, current flow in the fluid cancels the potential generated by fluid flow.

At the other extreme, if the fluid is poorly conducting, ‘back’ currents, also termed ‘volume’ currents flow in the surrounding region. If the region were homogeneous, magnetic fields would be generated by impressed currents only since the volume currents generate no net field.

The situation for finite flow in limited fault fractures more closely approximates the second case where the surface magnetic field is approximately given by:

$$B = \frac{\mu_0}{4\pi} \int_A \frac{j_i \times r}{r^2} \, dA$$

Reasonable fault models, in which fuid flows into a 200 m long rupturing fracture at a depth of 17 km, indicate that transient surface electric fields of several tens of millivolts per kilometer and transient magnetic fields of a few nT can be generated.

CHARGE GENERATION MECHANISMS

Numerous charge generation mechanisms have been suggested as potential current sources for electric and magnetic fields before and during earthquakes. These mechanisms include:

1) piezoelectric effects
2) triboelectricity effects produced by rock shearing
3) fluid disruption/vaporization
4) solid state mechanisms

Each of these has a solid physical basis supported by laboratory experiments on either dry rocks in insulating environments or single crystals of dry quartz. Each is capable of producing substantial charge under the right conditions.

However in reality, at least two fundamental problems need to be faced in the application of charge-generation processes to EM field generation in the Earth's crust.

a) the amplitude of each charge generation effect in wet rocks at temperatures and pressures expected in the Earth's crust (100º C, 100 MPa)

b) charge maintenance time and propagation in the conducting crust.

It's easy to foresee that a conductor (wet rocks) would not maintain charge separation…

MAGNETOHYDRODYNAMIC (MHD) EFFECTS

The induced magnetic field ***Bi*** generated by the motion ***v*** of a fuid with conductivity ***s*** in a magnetic field ***B0***, is governed by the equation:

$$\frac{\partial B}{\partial t} = \nabla \times v \times B + \frac{\nabla^2 B}{\mu_0 s} + \frac{\nabla s \times \nabla \times B}{\mu_0 s^2}$$

where $\boldsymbol{\mu_0}$ is the vacuum permeability. For low magnetic fields and low ***s*** values in the Earth"s crust where the fluid motion is not affected by the induced fields, the induced field is given approximately by the product of the magnetic Reynolds number ***Rm*** and the imposed field $\boldsymbol{B_0}$, i.e.,

$$B_i \approx R_m \times B_0 \approx \mu s v\, d B_0$$

where ***d*** is the length scale of the flow.

Critical parameters here are the likely flow velocities and fluid electrical conductivities in the crust.

Flow velocity is determined by rock permeability and fluid pressure gradients according to Darcy's Law.

It is diffcult to have flow velocities of more than a few mm/s with this mechanism.

Furthermore, fluid conductivities are unlikely to exceed that of sea water ($\approx 1 Sm^{-1}$).

Using these numbers, fluid fow in fractured fault zones at seismogenic depths (5 km) with a length scale of 1 km could generate transient fields of about 0.01 nT. Far too small to be observed at the Earth's surface.

Fields of a few nT are observed with waves in the ocean where the conductivity is $1 Sm^{-1}$ and wave velocities exceed 1 m/s…

THERMAL REMAGNETIZATION AND DEMAGNETIZATION

Crustal rocks lose their magnetization when T exceeds the Curie Point (580° C for magnetite) and become remagnetized again as the temperature drops below this value. At seismogenic depths near active faults, this process is unlikely to contribute to rapid changes in local magnetic fields since the thermal diffusivity of rock is typically $10^{-6} m^2 s^{-1}$ and migration of the Curie Point isotherm by conduction cannot be as much as a meter in a year.

At shallow depths in volcanic regions, particularly in recently emplaced extrusions and intrusions, thermal cracking with gas and fluid movement can transport heat rapidly and large local anomalies can be quickly generated.

These anomalies can be modeled as a magnetized slab in a half-space. Good examples of magnetic modeling of anomalies generated by cooling of extrusions are found in several cases. Some seasonal variations may result from annual temperature diffusion into magnetic rocks in the upper few meters of the Earth’s crust.

BASIC EM MEASUREMENT CONSTRAINTS

Against the natural background noise, **transient magnetic fields** can be reasonably measured to several nT, over months, to 1 nT, over days, to 0.1 nT, over minutes, and 0.01 nT, over seconds. Long-term changes and field offsets can be determined if their amplitudes exceed about 1 nT.

Comparable **electric field noise** limits are 10 mV/km, over months, several mV/km, over days, 1 mV/km, over minutes and 0.1 mV/km over seconds. EM noise increases approximately linearly with site separation.

Cultural noise further complicates measurement capability because of its inherent unpredictability. As well known this largely precludes measurements in urban areas.

At lower frequencies (microHertz to Hertz) for both electric and magnetic field measurements, a good technique involves the use of reference sites with synchronized data sampling in arrays using site spacing comparable to the expected source sizes (few km). Further improvements with noise reduction techniques such as adaptive fltering, etc…

CLASSICAL RESULTS FROM SCIENTIFIC LITERATURE

Electric, magnetic, and electromagnetic fields during and preceding earthquakes. Usual terms: seismomagnetic (SM) and seismo-electric (SE) effects. Those preceding earthquakes, or occurring at other times, are termed tectonomagnetic (TM) and tectonoelectric (TE) effects.

If reliable magnetic and electric field observations (i.e., those unaffected by seismic shaking) are indeed source related, clear offsets should occur at the time of large local earth-quakes because **the primary energy release occurs at this time.** These offsets should scale with the earthquake moment (size) and source geometry.

In fact, co-event observations provide a determination of stress sensitivity since the stress redistribution and the source geometry of earthquakes are well-determined.

GOOD SENSE…

With the coseismic calibration, tectonomagnetic and tectonoelectric effects can be quantifed and spurious effects identifed. Observations without consistent and physically sensible coseismic effects should generally be considered suspect.

The following examples are restricted to the strongest cases: data recorded independently on more than one instrument, data that are independently supported by other stable geophysical measurement systems, and data for which noise levels have been quantifed.

Reported measurements made with single instruments or time histories of measurements showing data only for a short period before earthquakes with some pre-cursive feature but no coseismic signals, should generally be considered not reliable.

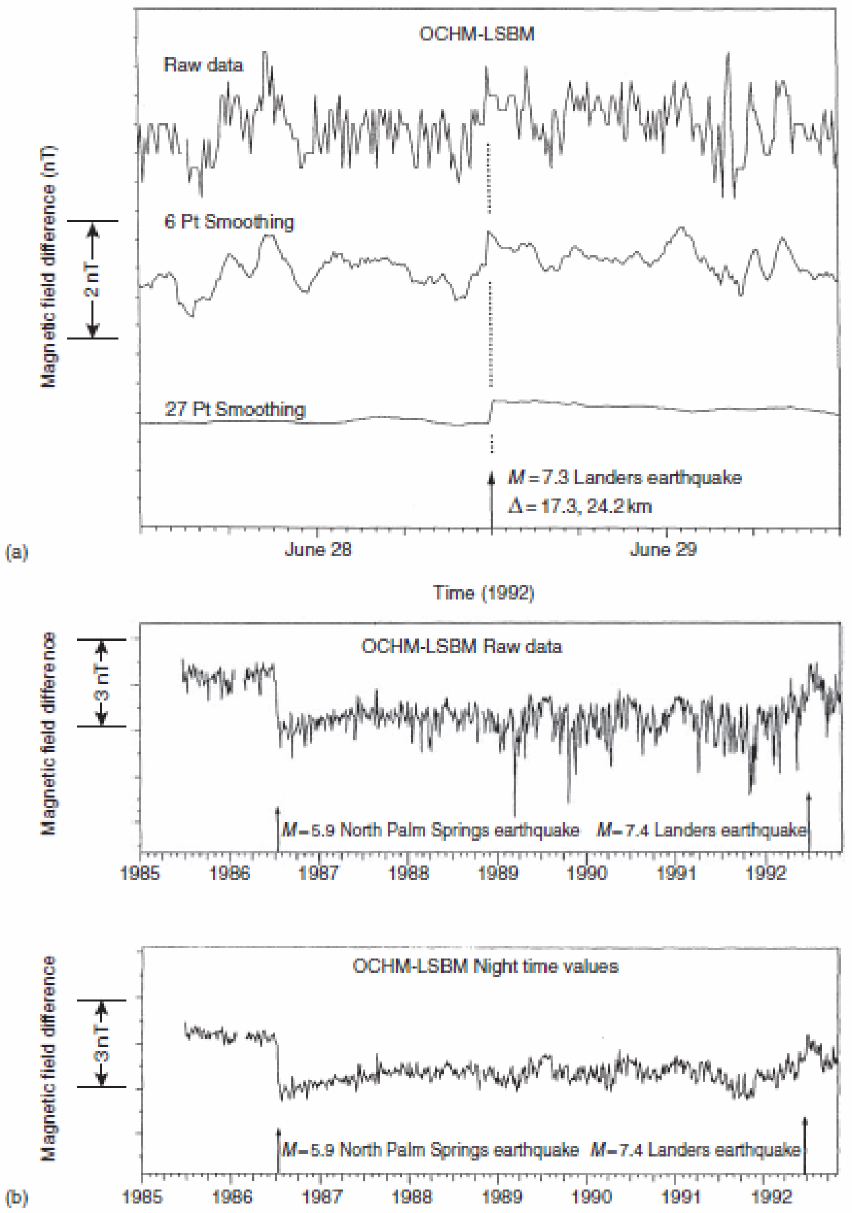

FIGURE 5 (a) Magnetic field differences between OCHM and LSBM (for location see Fig. 4) on the day before and after the Landers earthquake. (b) Similar magnetic field differences from 1985 through 1992 showing the occurrence times of the July 1986 $M = 6$ North Palm Springs earthquake and the June 1992 Landers earthquake (from Johnston *et al.*, 1994).

28th July 1992, Landers Earthquake
1.1 10^{27} dyne cm, Ml 7.3, two mags at 17 and 24 km from epicenter.

Comparison with Palm springs 1986 M 6 earthquake raw data and nightime.

Note that there is no indication of diffusion like character in the magnetic field offsets that can indicate that these effects are generated by fluid flow, nor that low frequency magnetic noise preceding the earthquake…

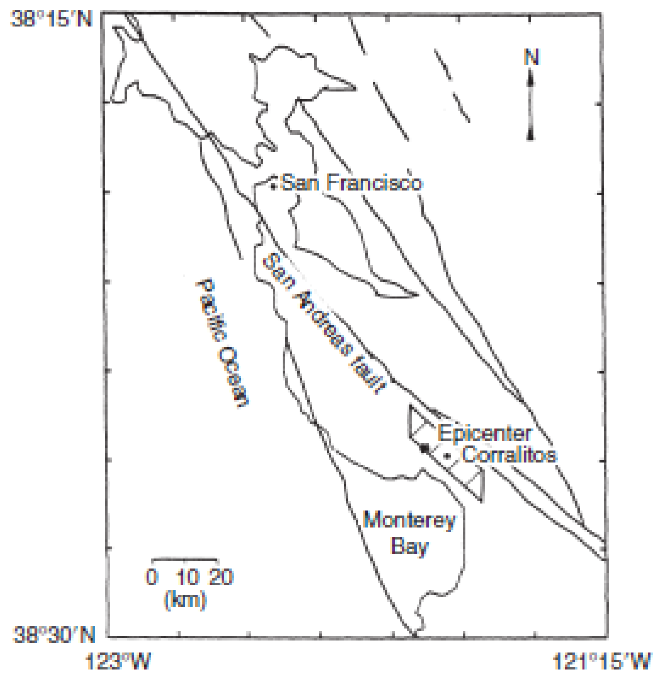

FIGURE 7 Location of ULF receiver at Corralitos, 7 km from the epicenter of the 18 Oct. 1989 $M = 7.1$ Loma Prieta earthquake. A second receiver was located at Stanford University (from Fraser-Smith *et al.*, 1990).

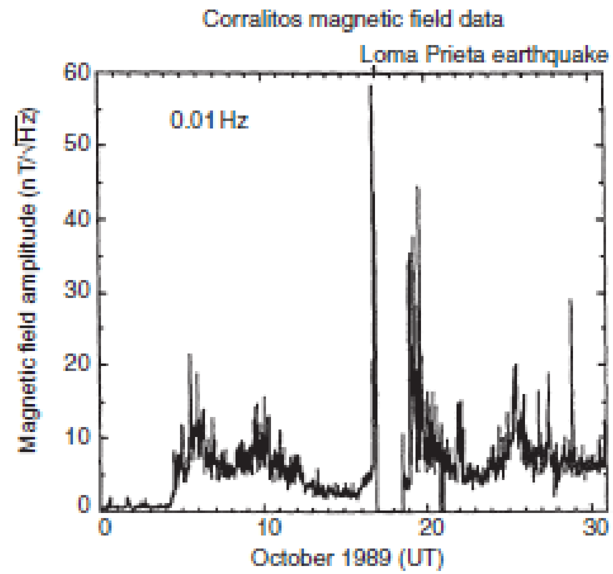

FIGURE 8 Magnetic field amplitude as a function of time during the 17 days before and 14 days after the Loma Prieta earthquake at 00:04 on 17 Oct. 1989 (from Fraser-Smith *et al.*, 1990).

Magnetic field measurements in the ULF band have a classical example in the famous M=7.1 Loma Prieta 18th October 1989 earthquake. A station 7 km from epicenter showed increased ULF noise up to 1.5 nT. It was observed 2 weeks and a few hours before. Magnetohydrodynamic and elektrokinetic origins were proposed as a cause.

These recordings are a sort of unique documented evidence for ULF. Similar records by ULF measurements were not obtained afterwards (M=6.7 Northridge, M=7.3 Landers and in Turkey M=7.4 Izhmet…)

Tectonoelectric phenomena

In China prior the 1976 Haicheng eq. and at Palmadele, in California (San Andreas Fault Zone) the most famous tectonoelectric phenomena related to earthquakes were reported.

Tectonoelectric phenomena related to earthquakes have been studied in Greece and Japan. Short-term geoelectric field transients (SES) of particular form and character should precede earthquakes with M > 5 at distances up to several hundreds of kilometers.

These transients appear to have a spatially uniform source field on the scale of the array but no clear corresponding magnetic field transients and no sensible coseismic effects. The SES have been empirically associated with subsequent distant earthquakes and claimed as precursors (VAN,Varotsos et al.,1996…).

These SES were suggested to preceed an M=6 .6 eq on 13/5/1995 at Chalkidiki some 83 km distance from sensors. Also demonstration of statistical significance is controversial…

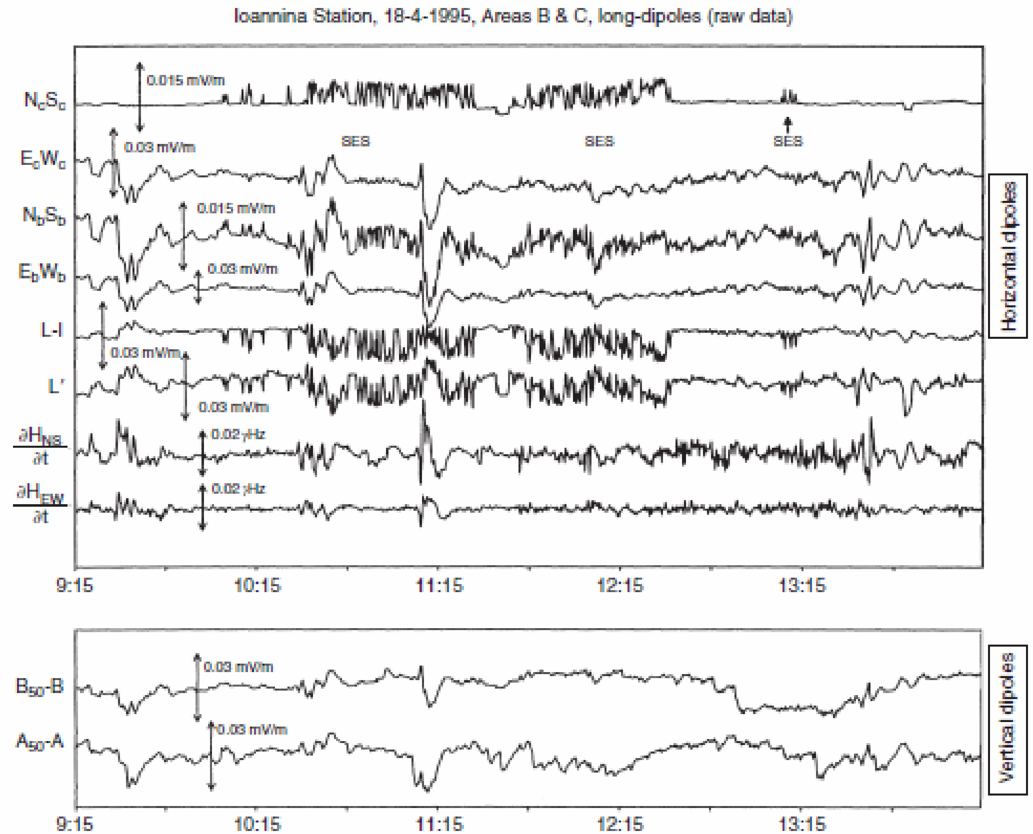

FIGURE 9 Observed SES recorded on multiple dipoles on 19 April 1995 at the Ioannina Station. Simultaneous measurements of magnetic field gradient are shown in the lower two plots (from Varotsos *et al.*, 1996).

Not very clear physical explanations describing how the SES signals are earthquake generated, are furnished. Moreover no coseismic effects related to the much larger earthquake source are observed. These observations are extremely controversial…

Other study of the SES recordings indicates that the SES signals have the form expected from rectification/saturation effects of local radio transmissions from high-power transmitters on nearby military bases…

High Frequency

Another enigma concerns the generation of high-frequency (>1 kHz) electromagnetic emissions associated with subsequent moderate earthquakes but, again, with no coseismic effects. Such emissions are reported to have been detected at great distances from these earthquakes and by magnetometers onboard satellites. However, the statistical significance of these observations is under dispute.

The generation of high-frequency electromagnetic radiation can be easily demonstrated in controlled laboratory experiments involving rock fracture in dry rocks. However, the Earth’s crust in seismically active areas is quite conducting (0.3–0.001 S/m) and propagation of VHF electromagnetic waves even on short distances through the crust is difficult to justify physically.

Propagation from earthquake source regions (5–50 km in depth), and in some cases through oceans with conductivities of 1 S/m, is physically implausible.

Parkfield, experiment and… earthquake...

On September 28, 2004 a Magnitude 6.0 earthquake struck Central California near the town of Parkfield… The quake caused no injuries and minimal property damage, but was of great interest to American geologists.

In 1984 the United States Geological Survey predicted that a Magnitude 6 earthquake would occur on the San Andreas fault near Parkfield within five years of 1988. The prediction was based on a sequence of 6 similar earthquakes that occured every 22 years (on average) from 1857 to 1966.

Although the 2004 Parkfield earthquake occured over a decade later than predicted, its magnitude and behavior fulfilled the prediction. In anticipation of this earthquake, geologists placed a large and varied suite of instruments along the Parkfield segment of the San Andreas Fault.

Sites – M6 Parkfield Earthquake

- Magnetic, Electric field and MT sites span the rupture of the 2004 M6 Parkfield earthquake
- High-resolution borehole strain and ground displacement sites also span the rupture.
- MT, strain and displacement data are sampled at 40 sps and 100 sps before, during and after the earthquake. Magnetic data are sampled at 0.002 seconds.

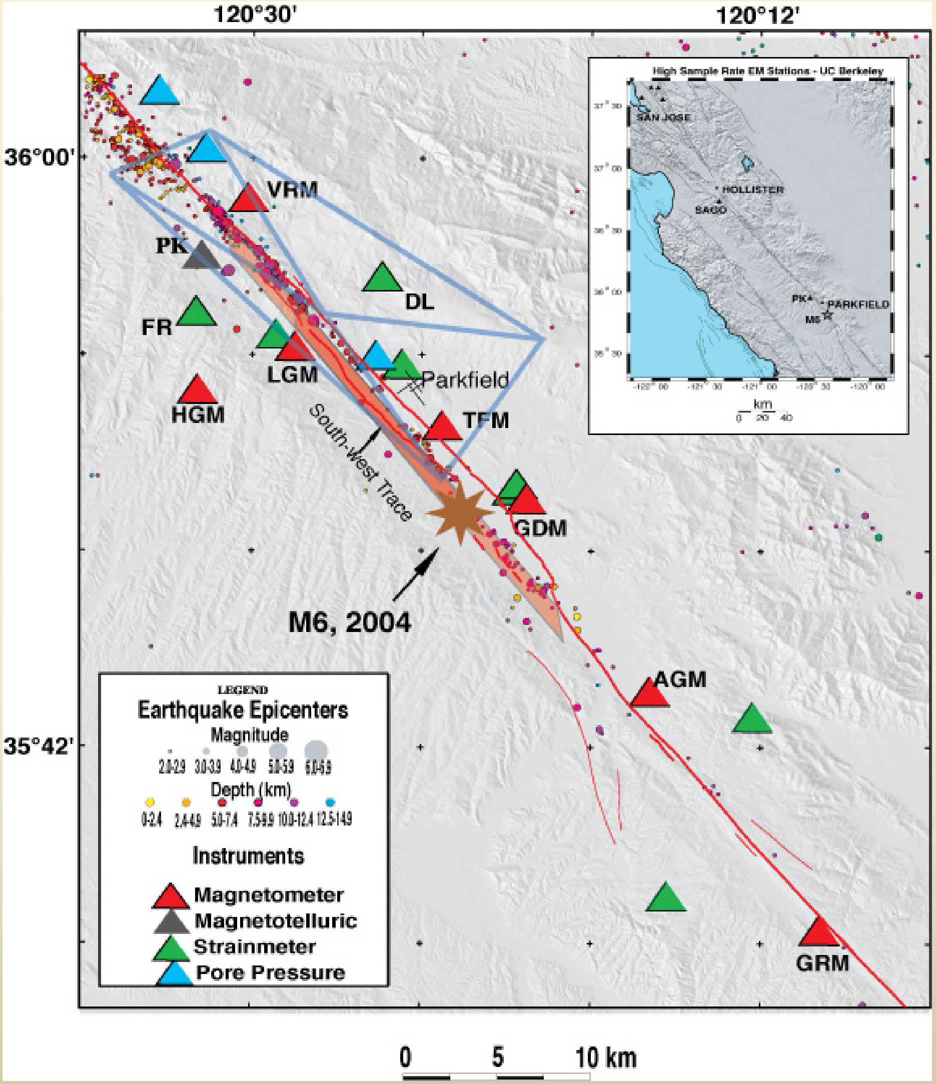

EM Signals with Earthquakes

- Expect EM signals
  - Immediately during Nucleation and Rupture Propagation as radiated EM – travels at speed of light but are rapidly attenuated in highly conductive fault zone regions. Observed in laboratory and with nuclear and conventional explosions but rarely reported for earthquakes.
  - With radiated Stress Waves and Co-seismic Static Stress Change – travel at seismic wave propagation speeds.
  - As second order effects from Ground shaking/rotation of EM instruments. Minimal if instruments installed in boreholes but problematic if instruments installed in weak sedimentary materials subject to strong ground motion.
  - Maybe at other times – but not substantiated.

Magnetic Field Offsets Resulting from the Earthquake Stress Drop of the M6 Parkfield Earthquake

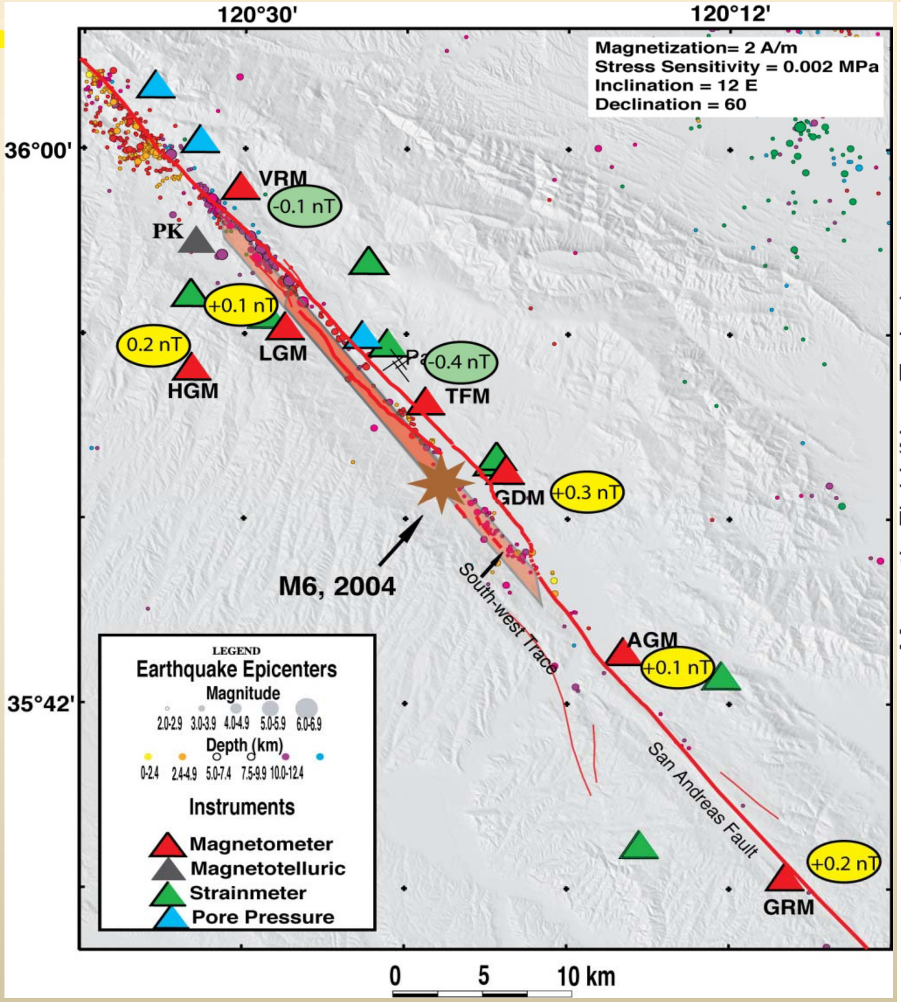

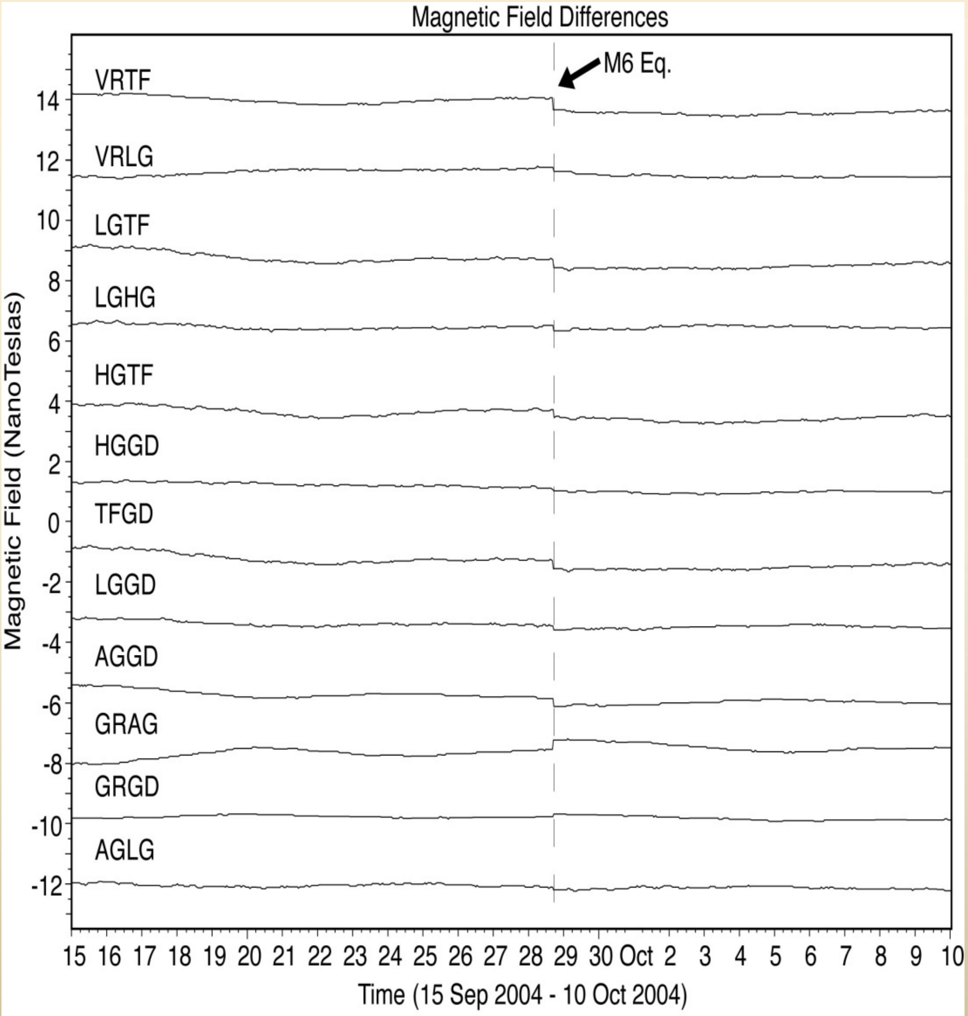

Magnetic/Geodetic Models from Earthquake Stress Drop

Observed and calculated magnetic field from magnetic/geodetic model

- -General Agreement
- -Overall, models quite tightly constrained
- -Fault slip process is thus generally well understood.

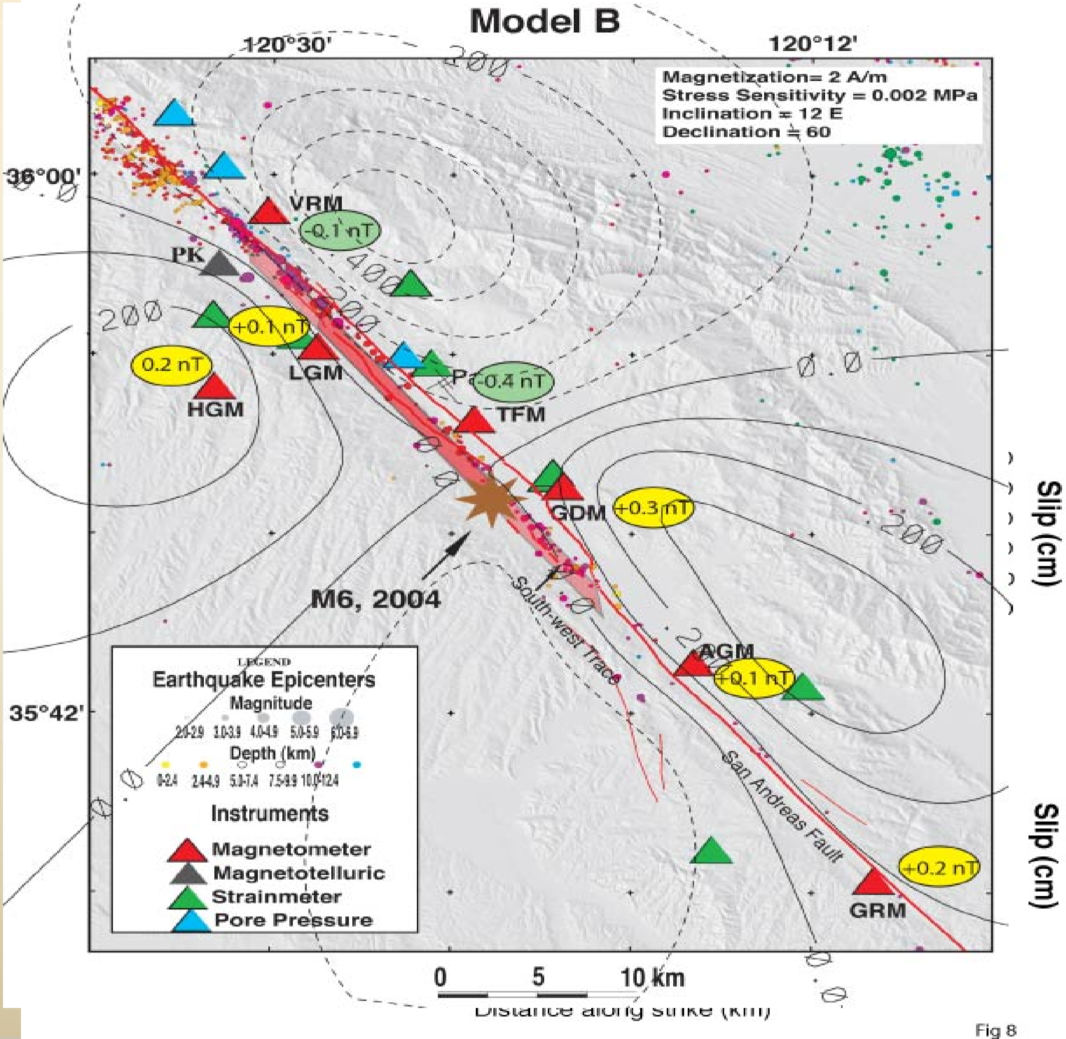

See BSSA, V96, S206-220, 2006

ITALY

The locations of the INGV tectonomagnetic network stations reported together with faults distribution in Central Apennines. (Adapted from the INGV-GNDT map of active faults in Central Italy).

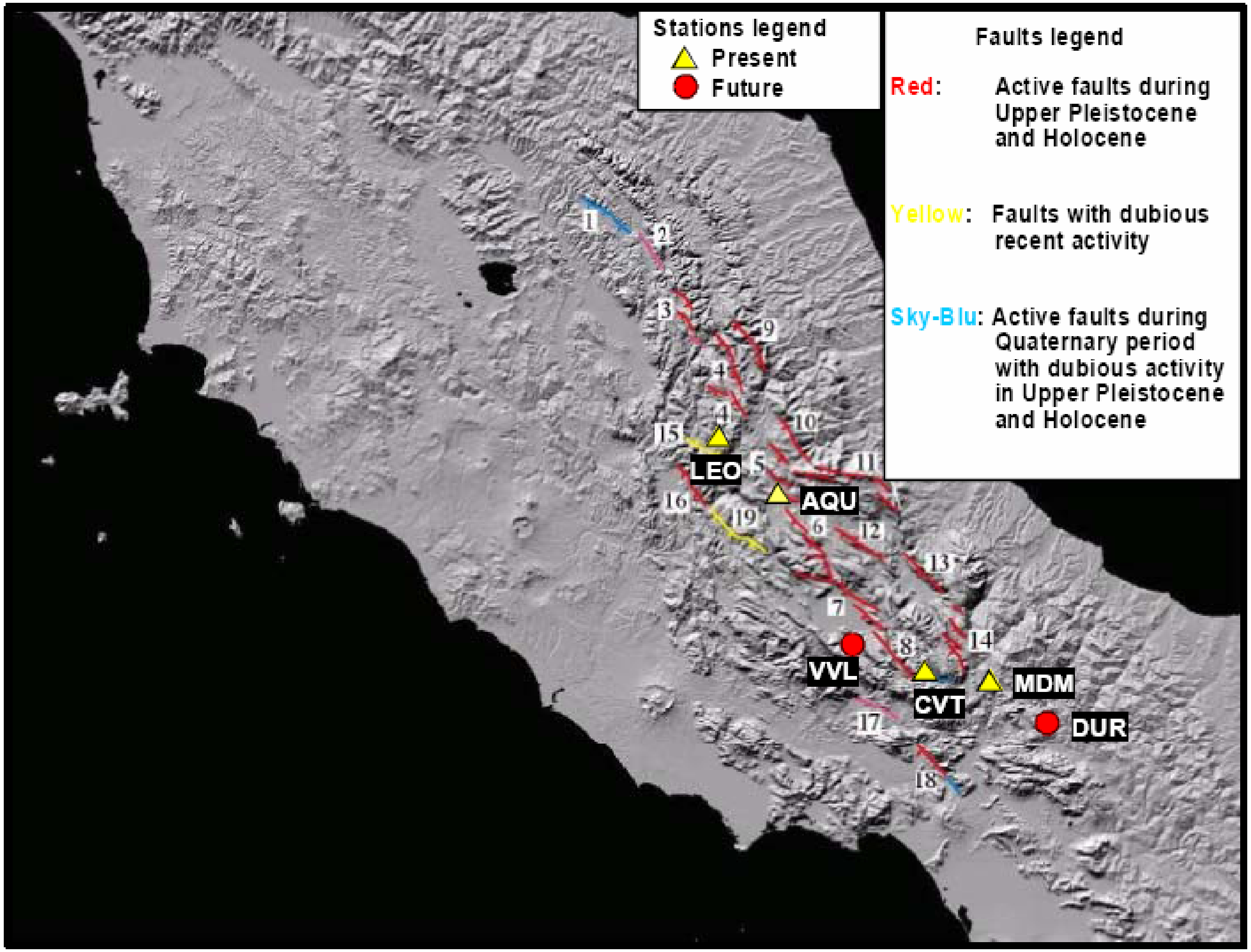

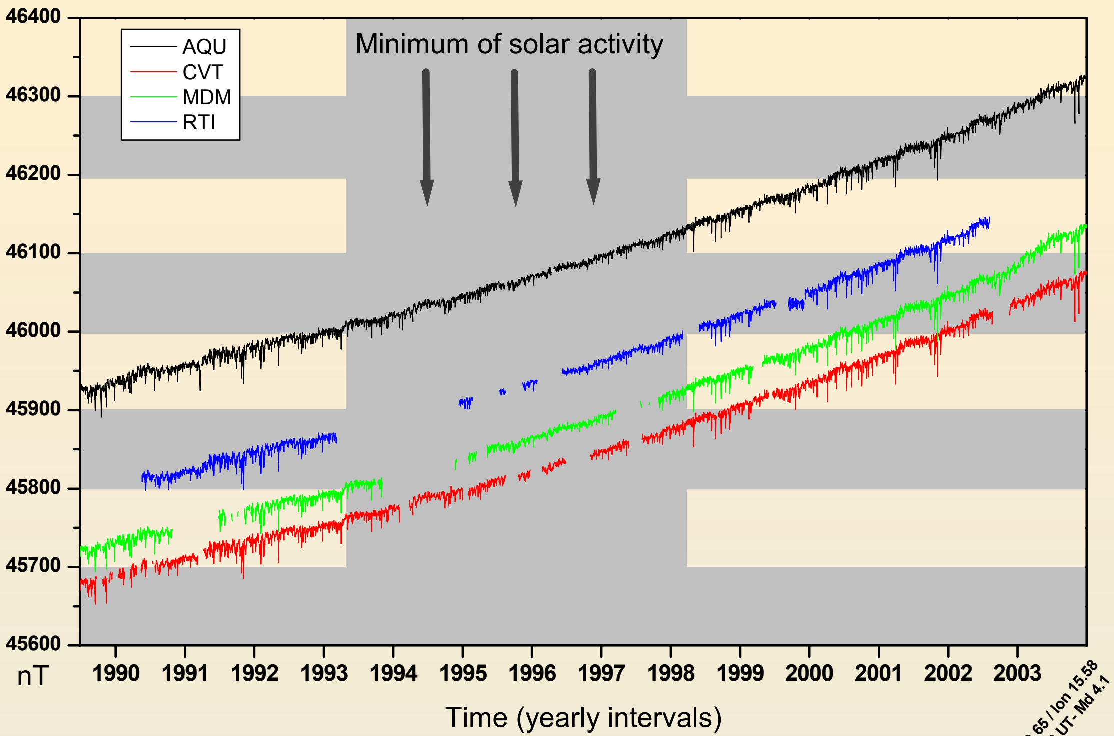

Registrazione dei segnali magnetici in Italia centrale (1989-2003)

Sebbene in presenza di moderata attivita' sismica e di qualche debole anomalia magnetica non e' facile identificare una relazione univoca tra anomalie magnetiche ed eventi sismici (o tettonici)

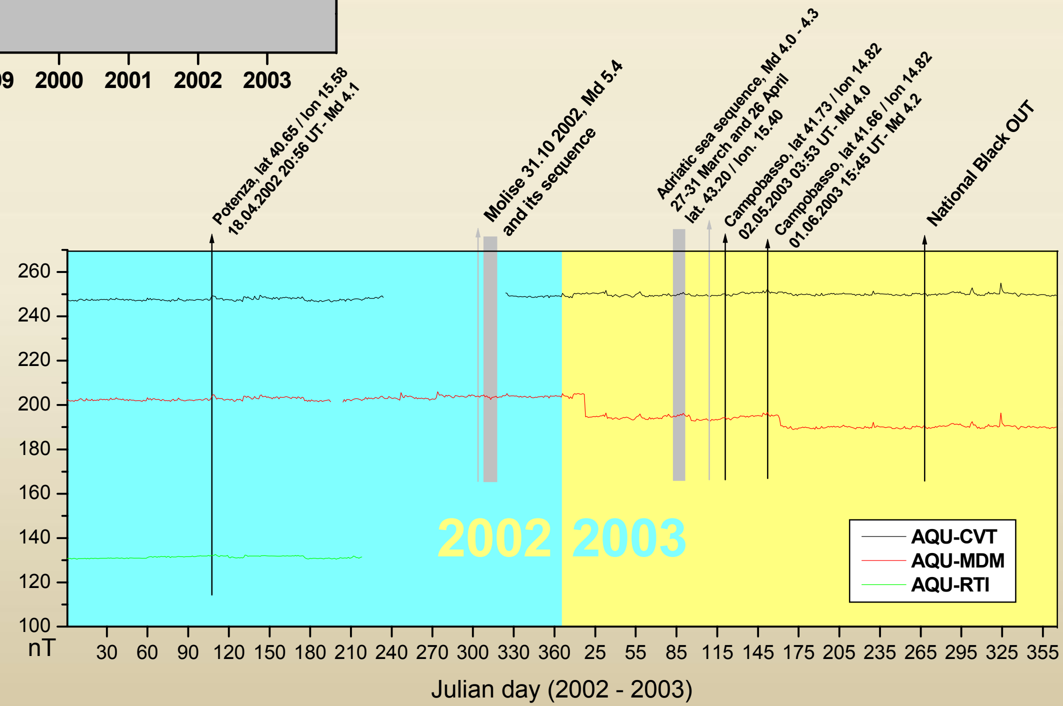

Differences (in nT) between couples of stations and main events

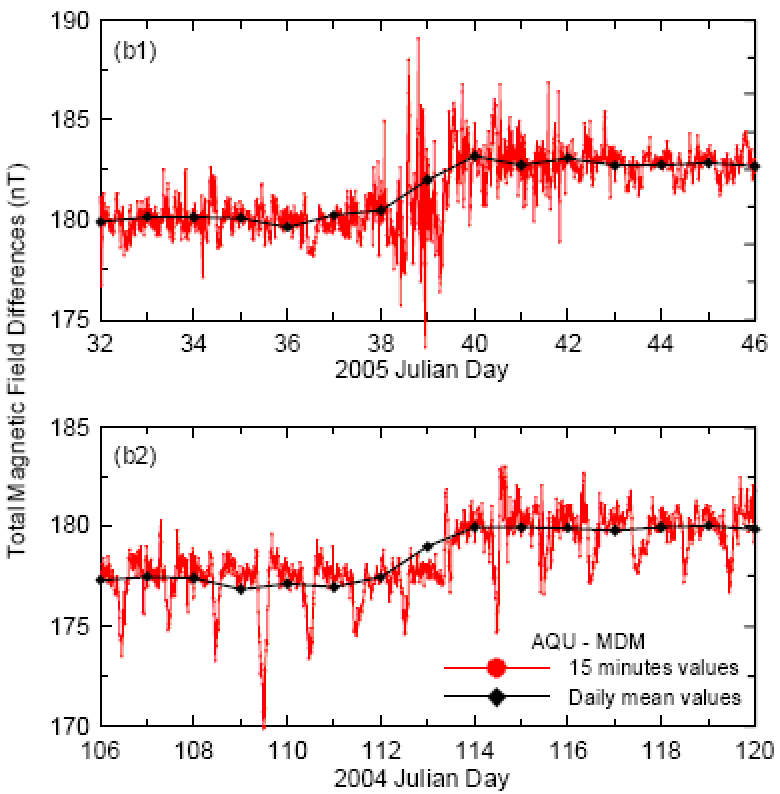

Both events show a jump of 2.5 nT in the differences AQU-MDM during 2 days. At the moment, there is no reasonable explanation for these events.

L'Assenza di chiare relazioni a eventi sismici nell'area e' stata confermata negli anni 2004 e 2005 anche se ci sono state e occasioni in cui si sono presentati eventi 'magnetici' non facilmente spiegabili.

…Moreover, in the differences involving the MDM station dataset are shown some events with no reasonable explanation at this moment. More investigation is needed for a correct interpretation of these events…

During 2007, two Ml 4 earthquakes occurred in proximity of two stations of the Italian network. Magnetic anomalies in the geomagnetic field that could be related with these tectonic events were observed. The maximum amplitudes of the anomalies are about 0.5 nT...

Osservazioni VLF presso L'Aquila (1997)

La variazione dei segnali elettromagnetici naturali nella banda VLF è registrata mediante due antenne search-coil nel range 15-40 kHz con 4 filtri passa-banda centrati a 15, 20, 30 and 40 kHz. Sensibilità strumentale: 200 fT at 40 Hz, sampling rate: 1 Hz, mediato a 20 s (12 bit resolution).

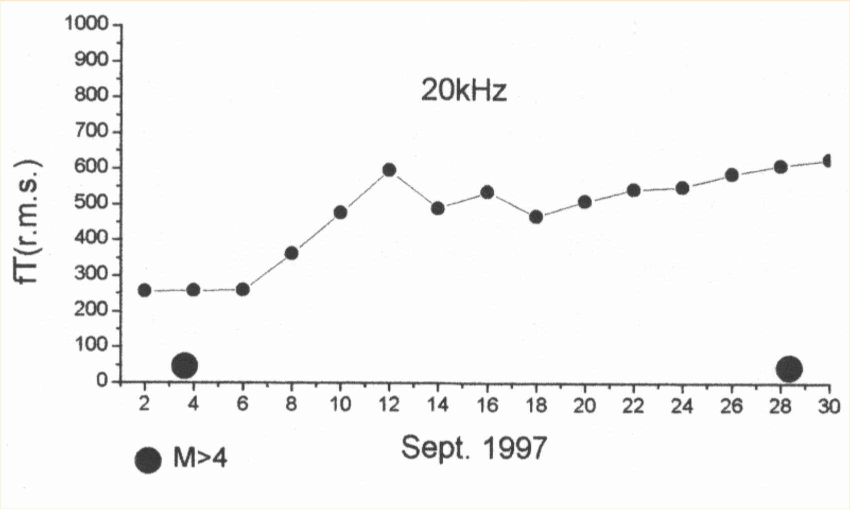

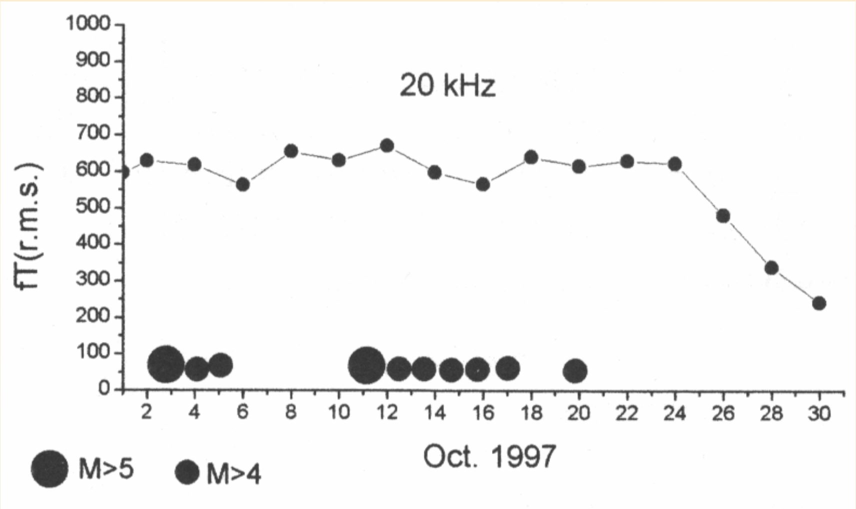

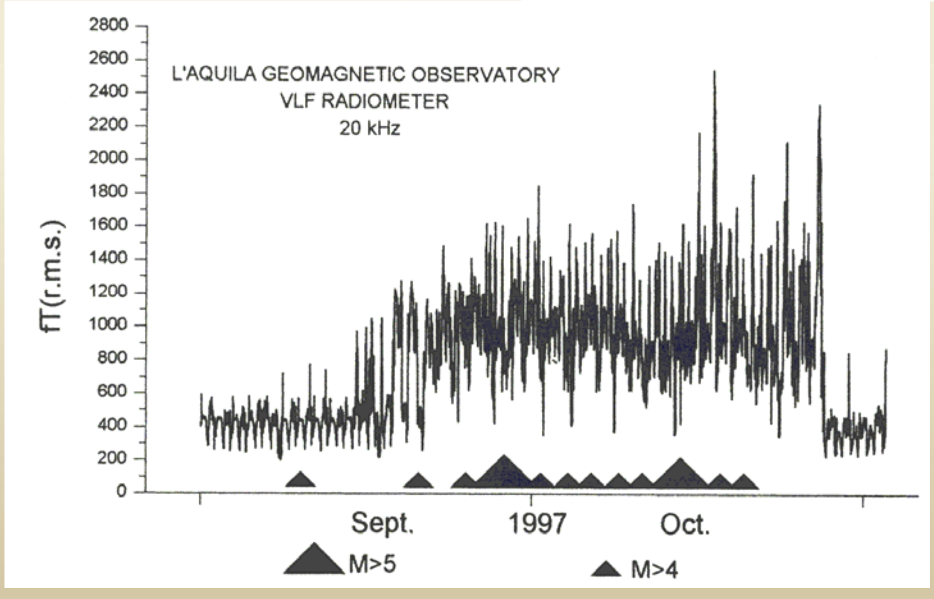

Lithosphere-Atmosphere-Ionosphere coupling

Some authors claim the existence of atmospheric-ionospheric anomalies before earthquakes.

Atmospheric electric field generated on or near the ground surface during the preseismic period may be caused by ions generated from radon emissions. Also positively charged holes, associated with microfracturing prior to earthquakes, diffuse from the focal zone to the ground surface. However, such preseismic electric fields on the ground followed by preseismic ionospheric anomalies have not yet been observed.

Also atmospheric gravity waves can propagate up and disturb the ionosphere before earthquakes. As proposed sources of gravity waves are long-period ground oscillations or thermal anomalies. This linkage is inferred from the observations of coseismic ground vibrations and tsunami-exciting atmospheric gravity waves which propagate into the ionosphere.

However, there is no report of preseismic long-period ground oscillations being detected, even by sensitive superconducting gravimeters. Some reports claim the existence of preseismic rises of temperature, infrared radiation, and surface latent heat flux, but none has explained how such anomalies can disturb the ionosphere through the atmosphere.

Lithosphere-atmosphere ionosphere coupling

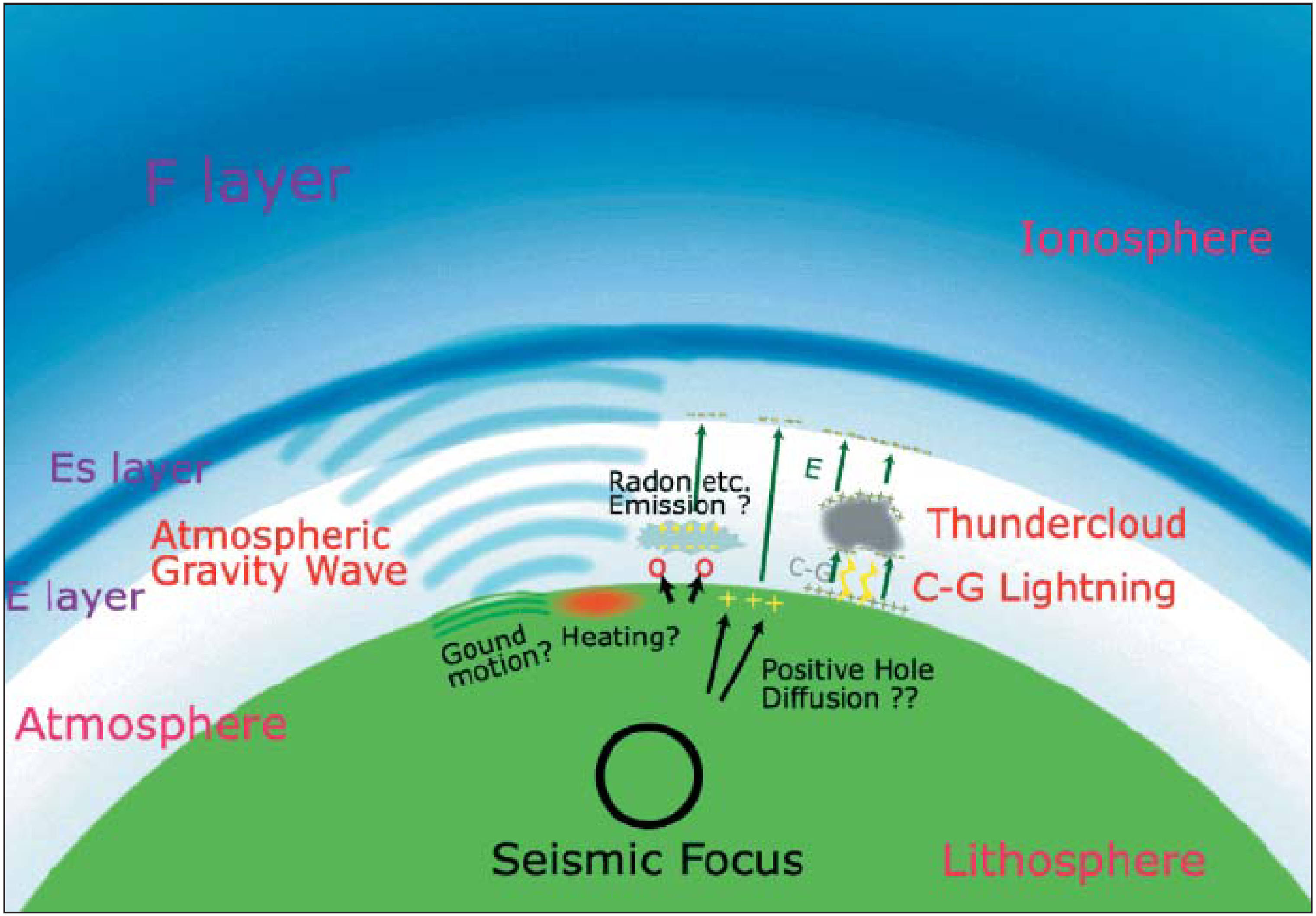

Fig. 2. Diagram of preseismic lithosphere-atmosphere-ionosphere coupling models and proposed mechanisms.

CONCLUSIONS…

Perturbations of EM fields in the epicentral regions of earthquakes are observed (probably less frequently than what reported in the literature…)

A variety of physical mechanisms can be used to explain these observations.

Co-seismic effects are easier to understand but also pre-sesmic EM effects are possible.

More work is certainly necessary and a fruitful approach should take in consideration…

1. Inclusion of constraints on the various physical mechanisms and models of various processes that are imposed by data from other disciplines such as seismology, geodesy, etc.
2. Demonstration of self-consistency in observations;
3. Determination and inclusion of realistic signal-to-noise estimates.
4. Identification of local noise sources.
5. Checking the implications of these data in other geophysical data obtained in the area. Unusual records can no longer be claimed as precursors just because they precede, or correspond approximately in time, to some local or distant earthquakes. They must be consistent with high-precision seismic and deformation data simultaneously obtained in the near field of each of the earthquakes.
6. Use of reference stations to quantify and remove common-mode noise generated in the ionosphere/magnetosphere.
7. Isolation of the most likely location of signal sources in the Earth's crust consistent with all available data. This appears to be particularly neglected in recent associations of ULF/VLF data with earthquakes.

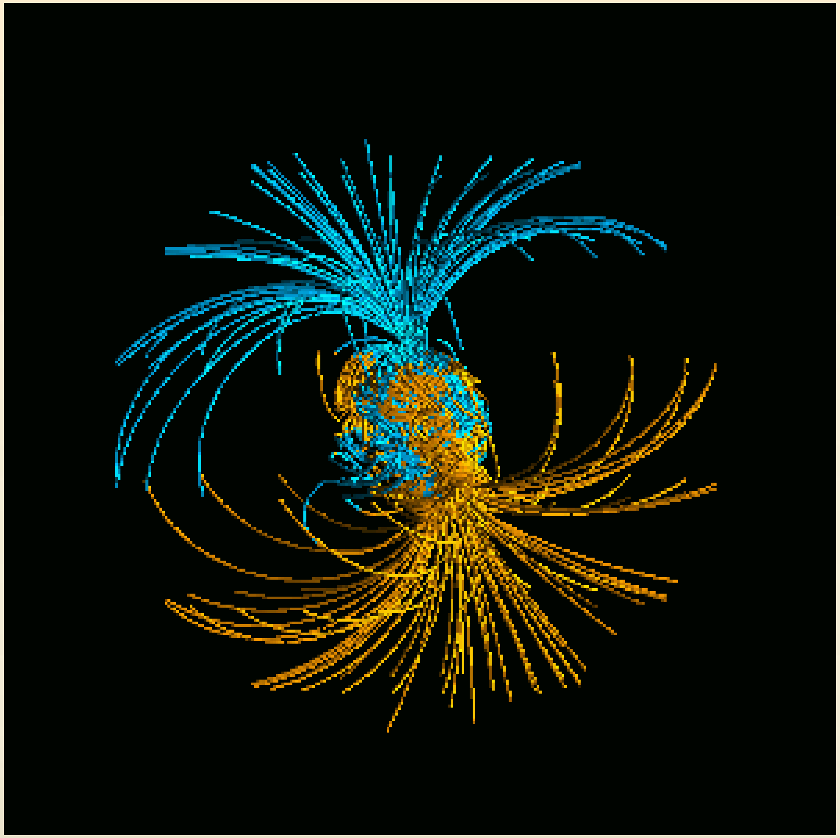

Grazie per l'attenzione …